Heliyon 10 (2024) e28986

Contents lists available at ScienceDirect

Heliyon

journal homepage: www.cell.com/heliyon

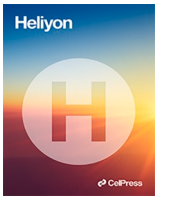

Research article

Investigation of flow behaviour in the nozzle of a Pelton wheel: Effects and analysis of influencing parameters

Satish Geeri [a], Aditya Kolakoti [b,j], Olusegun David Samuel [c,f,*], Mohamed Abbas [d], Peter Alenoghena Aigba [c], Habeeb A. Ajimotokan [e], Christopher C. Enweremadu [f], Noureddine Elboughdiri [g,h], M.A. Mujtaba [i]

[a] *Department of Mechanical Engineering, Pragati Engineering College, Surampalem, 533437, India*
[b] *Department of Mechanical Engineering, Raghu Engineering College, Visakhapatnam, 531162, India*
[c] *Department of Mechanical Engineering, Federal University of Petroleum Resources, Effurun, P.M.B 1221, Delta State, Nigeria*
[d] *Electrical Engineering Department, College of Engineering, King Khalid University, Abha, 61421, Saudi Arabia*
[e] *Department of Mechanical Engineering, University of Ilorin, Ilorin, Nigeria*
[f] *Department of Mechanical Engineering, University of South Africa, Science Campus, Florida, South Africa*
[g] *Chemical Engineering Department, College of Engineering, University of Ha'il, P.O. Box 2440, Ha'il, 81441, Saudi Arabia*
[h] *Chemical Engineering Process Department, National School of Engineers Gabes, University of Gabes, Gabes, 6029, Tunisia*
[i] *Department of Mechanical Engineering, University of Engineering and Technology, New Campus Lahore, Lahore, 54890, Pakistan*
[j] *Faculty of Engineering and Quantity Surveying, INTI International University, Persiaran Perdana BBN, Putra Nilai, 71800, Nilai, Negeri Sembila, Malaysia*

ARTICLE INFO

Keywords:
Pelton turbine
Taguchi
TOPSIS
GRA
CRITIC
DoE
Optimization

ABSTRACT

The performance of a Pelton wheel is influenced by the jet created by the nozzle. Therefore, a Computational Fluid Dynamics (CFD) simulation was proposed. In this study, the significant output parameters (outlet velocity, outlet pressure, and tangential force component) and input parameters (different pressure and spear locations) were examined. In addition, the influencing parameters and their contributing percentages to the performance of the Pelton wheel were calculated using different optimisation techniques such as Taguchi Design of Experiments (DoE), Technique for Order of Preference by Similarity to Ideal Solution (TOPSIS), Grey Relational Analysis (GRA) and Criteria Importance Through Intercriteria Correlation (CRITIC). The effect of input factors on the output response was examined with DoE, and the results show that the inlet pressure had the most significant impact (97.38%, 99.18%, and 97.38%, respectively, for all different spear sites with a 99% confidence level). In terms of preference values, the TOPSIS and GRA results are comparable (best ranks for simulation runs #24 and #25 and least ranks for simulations #2 and #3, respectively). The CRITIC results for the pressure parameter are in good agreement with the Taguchi ANOVA analysis. The last spear location (5 mm after the nozzle outlet), with an inlet pressure of 413685 Pa generated the best result when employing the TOPSIS and GRA techniques. The outlet pressure of the nozzle was found to have a significant impact on the flow pattern of the Pelton Wheel based on the analysis of the CRITIC, Taguchi, and CFD results.

* Corresponding author. Department of Mechanical Engineering, Federal University of Petroleum Resources, Effurun, P.M.B 1221, Delta State, Nigeria.
E-mail address: samuel.david@fupre.edu.ng (O.D. Samuel).

https://doi.org/10.1016/j.heliyon.2024.e28986
Received 8 July 2023; Received in revised form 27 March 2024; Accepted 27 March 2024
Available online 4 April 2024

1. Introduction

The Hydraulic Turbines (HTs) are rotational machines that convert water's potential head into productive forms of energy, such as mechanical and electrical energy [1]. Hydropower infrastructure, also known as HTs, is one of the turbo-machineries available for electricity generation [2]. The most widely used HT is an impulse turbine. The Pelton wheel (PW) is one of the turbines utilised under high-pressure head [3]. The PW was invented in 1980, and the turbine produces power by utilising water momentum impinging on buckets mounted on the periphery. Despite its age, the PW design continues to improve to achieve better efficiency by modifying the runner design [4,5].

The injector, runner, and casing are the geometrical elements that determine the flow in the PT [6]. The injector is the mechanical component of the PT that allows for changing fluid flow and enables the conversion of potential energy into kinetic energy [6]. Typically, the PT's injector consists of an injector spear and a nozzle [7].The injector opening is set by varying the location of the spear relative to the nozzle [8]. The key features that affect the performance of such PTs include the bucket, runner, nozzle, casing, mass flow rate, nozzle diameter, head, shape, and operating conditions [9,10]. Additionally, the outlet pressure, outlet velocity, and tangential force components of the jet influence how the flow of the turbine's nozzle behaves. However, these phenomena might affect jet velocity distribution and shape, leading to undesired secondary flows, lowering the nozzle velocity coefficient, injector efficiency, and system efficiency. Hence, erosion is a matter of grave concern in the PT. Recently, a lot of effort has been put into employing optimization tools to better understand the PT's performance characteristics, the operating environment, and its variable design component [11,12]. The experimental and modelling properties of various types of PTs have been investigated using a variety of model techniques [13,14].

A variety of models have been employed to model the performance characteristics of PT, as summarized in Table 1. As observed, Box-Behnken Design of Experiments (BBDE), Taguchi & ANOVA, TOPSIS & PSI, RSM, Smoothed Particles Hydrodynamics (SPH), Direct Search Approach (DSA), FLUENT code (FC) have been employed in Turgo turbine (TT) [15], lab scale Pelton wheel (LPSW) [13], Pelton turbine buckets (PTBs) [16], floating blade water wheel turbine (FBWWT) [17], injector of the PT [18], Pelton turbine wheel (PTW) [19], static bucket of a Pelton turbine (SBPT) [20], respectively.

Reviewing the comprehensive studies revealed that the three robust models namely, Technique for Order of Preference by Similarity to Ideal Solution (TOPSIS), Grey Relational Analysis (GRA), Criteria Importance Through Intercriteria Correlation (CRITIC) have not been utilized to predict the performance characteristics, specifically the velocity of the runner with outlet pressure of the PT. The study aims to assess the impact of input parameters on the output parameters by determing their contribution percentages to identify the performance of the PW.

1.1. Mathematical relations of TOPSIS

TOPSIS concepts emphasize that the chosen alternative must be close to the positive ideal solution and far from the negative ideal solution. The ranks for the obtained solution were displayed using TOPSIS analysis [17]. The following processes are involved in these procedures:

Step 1: Consists of a decision matrix with 'n' attributes and 'm' possibilities, as shown in Eq. (1).

$$D_m = \begin{bmatrix} p_{11} & \cdots & p_{1n} \\ \vdots & \ddots & \vdots \\ p_{m1} & \cdots & p_{mn} \end{bmatrix} \tag{1}$$

Where P_{ij} represents the performance of the ith alternative with respect to the j^{th} attribute.

Step 2: The normalised matrix can be obtained by using Eq. (2)

$$r_{ij} = \frac{p_{ij}}{\sqrt{\sum_{i=1}^{m} p_{ij}^2}} \tag{2}$$

Table 1
An overview of modelling and simulation of flow behaviour in a Pelton turbine.

Type of Pelton turbine	Area of investigation: parameters/responses	Model tool(s)	Remarks	Refs.
PTs	Velocity distribution, pressure distribution, and jet spread/turbine efficiency (TE)	Nil	Enhanced TE resulted from the optimization of purposeful variables	Nedelcu et al. [6]
TT	Nozzle diameter, number of nozzles, jet impact location/turbine efficiency	BBDE	The capability of the BBDE was established for TT	Gallego et al. [15]
FBWWT	water flow rate, number of buckets, shape of the blade	Taguchi and ANOVA	Predictable optimum design was achieved using Taguchi	Permanasari et al. [17]
Pelton Turbine Buckets	Silt erosion, silt loaded factors/erosive wear rate variables (EWRV)	TOPSI and PSI	TOPSIS and PSI were detected as suitable for identifying EWRV	Thakur et al. [16]
SBPT	Head, jet incidence, and flow rate	FC	Stable flow was estimation realised from the optimization protocol	Zoppé et al. [20]

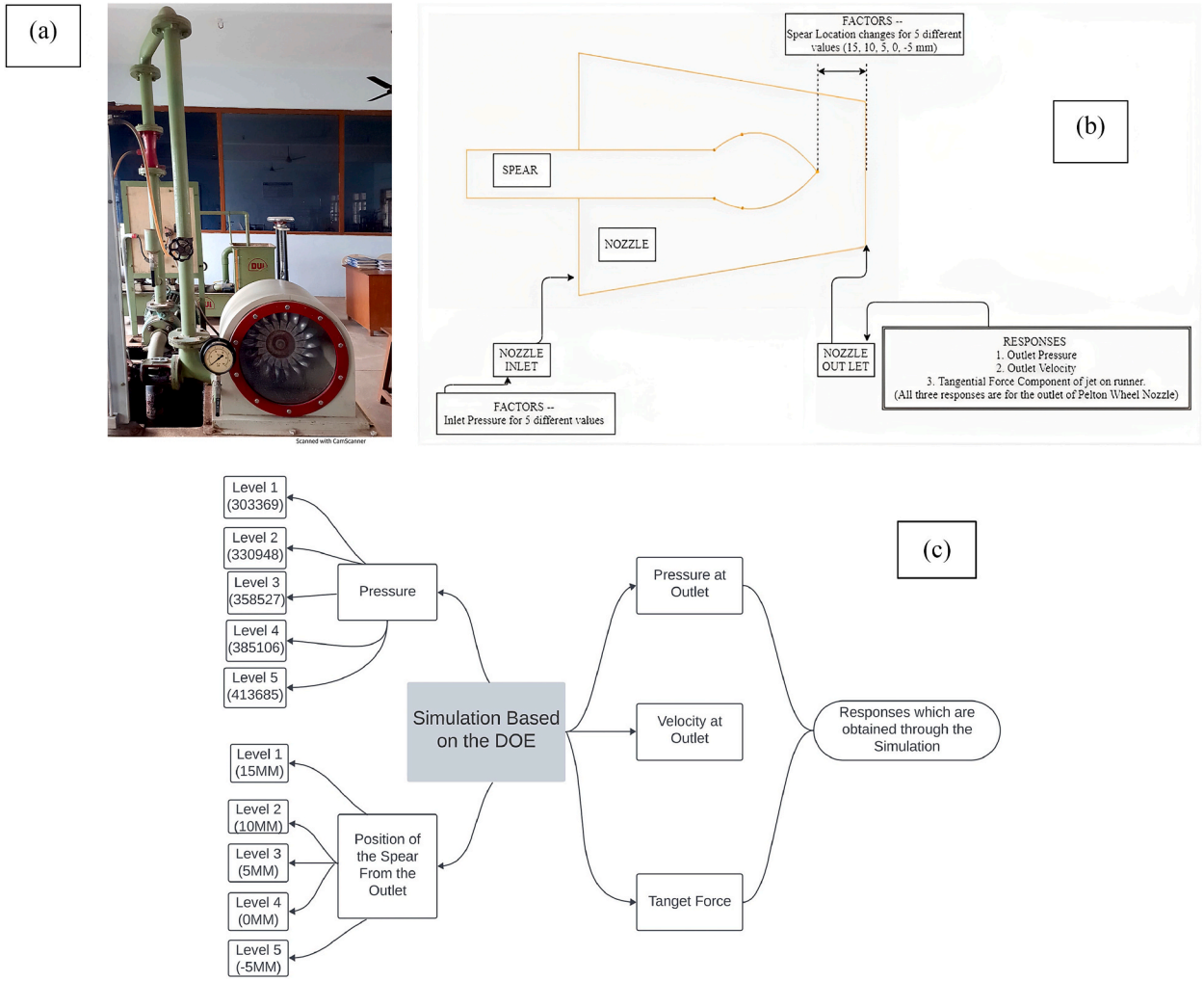

Fig. 1. Pelton wheel: (a) Experimental setup, (b) Flow chart for modelling, (c) Correlation between the input parameters and responses.

Step 3: The weighted normalised decision matrix, $U = [u_{ij}]$, can be determined using Eq. (3).

$$U = w_j r_{ij} \tag{3}$$

Where $\sum_{j=1}^{n} w_j = 1$ and W_j (j = 1,2, .., n) were considered to be the weight of each attribute.

Step 4: Positive ideal and negative ideal solutions are resolved with Eqs. (4) and (5), respectively

$$U^{+} = \left\{ \left(\sum_{i}^{max} u_{ij} \middle| j \in J \right), \langle \sum_{i}^{min} |j \in 1 | i = 1, 2, .., m \rangle \right\} = = \left\{ u_1^{+}, u_2^{+}, .., u_n^{+} \right\} \tag{4}$$

$$\mathrm{U}^{-} = \left\{ \left(\sum_{\mathrm{i}}^{\min} \mathrm{u_{ij}} | \mathrm{j} \in \mathrm{J} \right), \langle \sum_{\mathrm{i}}^{\max} |\mathrm{j} \in 1 | \mathrm{i} = 1, 2, .., \mathrm{m} \rangle \right\} = \left\{ u_1^{-}, u_2^{-}, .., u_n^{-} \right\} \tag{5}$$

Step 5: The separation of the alternative from the ideal solution and the separation from the negative solution are expressed using Eqs. (6) and (7), respectively.

$$S_i^{+} = \sqrt{\sum_{j=1}^{n} \left(u_{ij} - u_j^{+} \right)^2}, \mathrm{i} = 1, 2, ..\mathrm{m} \tag{6}$$

$$S_i^- = \sqrt{\sum_{j=1}^{n} \left(u_{ij} - u_j^-\right)^2}, \mathrm{i} = 1, 2, ..\mathrm{m} \tag{7}$$

Step 6: Determine the relative closeness of the distant alternatives to the positive ideal solution using Eq. (8).

$$P_i = \frac{S_i^-}{S_i^+ + S_i^+} \ \mathrm{i} = 1, 2, ..\mathrm{m} \tag{8}$$

Step 7:The P_i values were ranked in descending order to identify the set of choices with the highest preference.

1.2. Mathematical relations of Grey Relational Analysis (GRA)

GRA is a technique that employs grey system theory to solve multiple outputs with complex relationships [21]. The objective of exploring GRA is to scrutinise the qualitative and quantitative relationships between the inputs in order to recognise the dynamic characteristics of the process and their relative influences [22]. GRA commences by normalising experimental data from zero to one, a process known as grey relational generation. The grey relational coefficient, which represents the correlation between the desired and actual experimental data, is determined after normalising the data. The total grey relational grade for each response is then calculated by averaging the calculated grey coefficients. As a result, a multi-response problem is reduced to a single-response process optimisation problem with grey relational grade (GRG) as the objective function. Fig. 1 depicts the complete GRA procedure. Eqs. (9) and (10) were used for the "larger-the-better" and "smaller-the-better" conditions for the maximum expected data sequence and normalising response data that are in sequence, respectively.

$$X_i(P) = \frac{y_i(P) - min\ y_i(P)}{max\ y_i(P) - \min yi(P)} \tag{9}$$

$$X_i(P) = \frac{\max\ \ max\ y_i(P) - y_i(P)}{max\ y_i(P) - \min yi(P)} \tag{10}$$

Where $X_i(P)$ is generated by grey relational generation, $min\ y_i(P)$ is the least value of $y_i(P)$ for the P^{th} response and $\max y_i(P)$ is the highest value for the P^{th} response where P = 1, 2, … for various output responses considered in a sequence.

Grey relational coefficients are calculated between the reference data and the normalized data. The GRC is determined with Eq. (11).

$$\xi_i(P) = \frac{\Delta_{min} + \psi\ \Delta_{max}}{\Delta_{0i} + \psi\ \Delta_{max}} \tag{11}$$

Where $\Delta_{0i}(P) = |X_0(P) - X_i(P)|$, ψ is the distinctive coefficient lying between $0 \le \psi \le 1$, Δ_{min} is the minimum value for Δ_{0i} and Δ_{max} is the maximum value for Δ_{0i}.

The GRC can be calculated using Eq. (12). As shown in Eq. (12), n represents the number of output responses. The higher the value of GRC, the closer the subsequent parameter arrangement is to the optimal solution.

$$\gamma_i = \frac{1}{n} \sum_{i=1}^{n} \xi_i(P) \tag{12}$$

1.3. Mathematical relations of CRITIC

CRITIC is a weighting method based on objective criteria. This method considers not only the amount of information contained in the criteria, but also the contrast between different schemes and the conflict between the criteria, resulting in more objective and reasonable calculations [23,24]. The contribution percentages of the output parameters are computed using Eqs. 13–15. Steps 1–6 provide a summary of the estimated procedures required in adopting CRITIC.

Step 1: Normalise the decision matrix using Eq. (13)

$$\overline{X}_{ij} = \frac{X_{ij} - X_j^{worst}}{X_j^{best} - X_j^{worst}} \tag{13}$$

Step 2: Calculate the standard deviation for each criterion.

Step 3: Construct the symmetric matrix from which the linear correlation coefficients are estimated.

Step 4: Calculate the measure of conflict created by the criterion with respect to the decision situation, as expressed in Eq. (14)

$$\sum_{k=1}^{m} \left(1 - r_{jk}\right) \tag{14}$$

Step 5: Determine the quality of the information in relation to each criterion.

$$C_j = \sigma_j^* \sum_{k=1}^{m} (1 - r_{jk}) \tag{15}$$

Step 6: Determine the objective weights and weight percentages.

1.4. Taguchi method

The Taguchi method produces an outcome based on the Signal-To-Noise (S/N) ratio, which defines the difference between simulated and target data and is calculated from the mean to the standard deviation [25]. The S/N value is used in this analysis to represent the required value (mean) for the response and the unrequired value (standard deviation) [26]. This method is classified into three parameters based on the output value: medium is better, higher is better, and lower is better.

1.5. Computational Fluid Dynamics (CFD)

The numerical simulation of the Pelton turbine was done using CFD. With the aid of CFD, precise measurement has been obtained. For instance, Popovski et al. [27] claimed that the CFD analysis is very reliable and accurate with sufficient accuracy and precision for more complex applications, such as the flow in PTs' runner. Patel et al. [4] investigated the development of the PT using a numerical solution and explained the significance of Pelton turbine design optimization. The result described the turbine's performance in relation to each component. Vytvytskyi and Lie [28] emphasized the importance of a mechanistic model over an empirical model for the numerical analysis of Francis turbines. Empirical turbine models require numerous experiments on actual turbine models and cannot be directly applied to other systems. Mechanistic models, on the other hand, are simply based on Euler's equation but have distinct design parameters that must be evaluated. These design parameters are chosen using an algorithmic design rule based on available head and flow rate information.

1.6. Motivation, uniqueness, and research objectives

In this study, an attempt is made to investigate Taguchi DoE based TOPSIS and GRA, as well as a comparison of all four analyses, which is limited in the literature. Therefore, the primary goal of this work is to identify the optimal input variable that has the most significant influence on the output parameter, which, in turn, reflects the overall performance of the PW. Additionally, the current work aims to identify the best-influencing parameters on the overall performance of the PW. The overall performance of the PW is determined by the jet produced by the nozzle, which has an impact on the buckets. As a result, the current work focuses on the analysis of flow behavior in nozzles by changing input parameters (inlet pressure and spear location) and observing the effect on outlet pressure, velocity, and tangential force components. Later, the optimal influencing parameter for the corresponding variables of input parameters interms of output parameters was investigated using Taguchi, TOPSIS, GRA, and CRITIC analysis.

2. Governing equations in CFD

The exact k-equations contain various unknown and unmeasurable terms. The standard k-turbulence model [29] is utilised for a more practical approach as it is based on our best understanding of the relevant processes, minimising unknowns and providing a set of equations that can be applied to a wide range of turbulent applications [30]. The turbulent kinetic energy k, dissipation E, and eddy viscosity were modelled using Eqs. (16) to (18).

$$\frac{\partial(\rho K)}{\delta t} + \frac{\delta(\rho K \mu_i)}{\delta x_i} = \frac{\delta}{\delta x_i}\left[\frac{\mu_t}{\sigma_k}\frac{\delta K}{\delta x_j}\right] + 2\mu_t E_{ij} E_{ij} - \rho\epsilon \tag{16}$$

$$\frac{\partial(\rho \in)}{\delta t} + \frac{\delta(\rho \in \mu_i)}{\delta x_i} = \frac{\delta}{\delta x_j}\left[\frac{\mu_t}{\sigma_k}\frac{\delta \in}{\delta x_j}\right] + 2\, C_{ie}\frac{\in}{K} 2\mu_t E_{ij} E_{ij} - \rho C_{2e}\frac{\in^2}{K} \tag{17}$$

$$\mu_t = \rho C_\mu \frac{k^2}{\varepsilon} \tag{18}$$

Rate of change of k or ε in time + Transport of k or ε by advection = Transport of k or ε by diffusion + Rate of production of k or ε - Rate of destruction of k or ε.Here μ_i , E_{iJ}, μ_t represent velocity components in the corresponding direction, rate of deformation, and turbulent viscosity, respectively.

The equations also include some adjustable constants $\sigma_k, \sigma_\epsilon, C_{1\varepsilon}, C_{2\varepsilon}$. The values of these constants have been determined through numerous iterations of data fitting for a wide range of turbulent flows.

These are as follows : $C_\mu = 0.09 \sigma_k = 1.00 \sigma_\epsilon = 1.30 C_{1\varepsilon} = 1.44 C_{2\varepsilon} = 1.92$

2.1. Tangent force and the flow through nozzle

A nozzle is a short, gradually converging tube installed at the outlet and penstock to convert the total energy of the flowing water

Table 2
Factors and corresponding levels.

Factors	Units	Level 1	Level 2	Level 3	Level 4	Level 5
Location of Spear w.r.t Nozzle outlet	Mm	15	10	5	0	−5
Representation of Spear Location	Mm	1	2	3	4	5
Inlet Pressure	Pa	303369	330948	358527	386106	413685
Representation of Inlet Pressure	Pa	1	2	3	4	5

Table 3
Orthogonal array of process variables for the simulation process (Taguchi DoE).

S/N	Spear location	Inlet pressure	Outlet pressure	Velocity	Tangential force
	Mm	Pa	Pa	m/s	N
1	1	1	291205	24.72	51160.1
2	1	2	317681	25.81	55811.56
3	1	3	344156	26.87	60461.77
4	1	4	370632	27.88	65114.82
5	1	5	397108	28.86	69766.18
6	2	1	291142	25.04	52499.35
7	2	2	317612	26.15	57269.1
8	2	3	344082	27.22	62045.43
9	2	4	370553	28.25	66817.98
10	2	5	397023	29.24	71591.41
11	3	1	292815	24.97	52233.8
12	3	2	319437	26.08	56982.55
13	3	3	345936	27.14	61676.23
14	3	4	372549	28.16	66420.67
15	3	5	399162	29.15	71165.48
16	4	1	298499	25.08	52684.46
17	4	2	325637	26.2	57474.27
18	4	3	352775	27.27	62264.01
19	4	4	379913	28.29	67054.28
20	4	5	407051	29.29	71843.85
21	5	1	296235	25.41	54097.87
22	5	2	323168	26.55	59016.8
23	5	3	350100	27.63	63935.27
24	5	4	377033	28.67	68854
25	5	5	403965	29.68	73772.92

into kinetic energy. Nozzles are used to develop high-flow velocities. It is necessary for impulse turbines to convert all of the hydraulic energy into kinetic energy. The discharge is given by Eq. (19), while Eqs. (20) and (21) are used to account for the head at the nozzle and head losses in the nozzle, respectively [6,31].

$$Q = a_1 v_1 = a_2 v_2 \tag{19}$$

$$H = \frac{V^2}{2g} + \frac{P}{\rho} \tag{20}$$

$$H_l = H_2 - H_1 \tag{21}$$

3. Methodology

The experimental setup of the PW is shown in Fig. 1(a), and the specifications are as follows: rated supply head 30 m, discharge 500 mm, normal speed 1000 rpm, jet diameter 22 mm, throat diameter 29.58 mm, and pump rated head 35 m. The PW's geometry, a modelling flowchart, and the relationship between the input parameters and response are all displayed in Fig. 1(b–c). For the 2D design and simulation, the ANSYS software was utilized (see section 2). Boundary conditions are assigned in the ANSYS program utilizing Table 2 as a guide for the produced 2D geometry. In the simulation, the k-ξ turbulent model serves as the governing equation. CFD modelling is needed to predict the fluid flow under PW. Fluid velocity was necessary for the impact to manifest on the buckets. Given this, the simulation was run using the database for the simulation process shown in Table 3.

4. Results and discussion

The objective of this study is to determine the optimal influencing input and output parameters on the overall performance of the PW. The overall performance of the PW depends on the water jet from the nozzle, which impacts the buckets. Therefore, this study

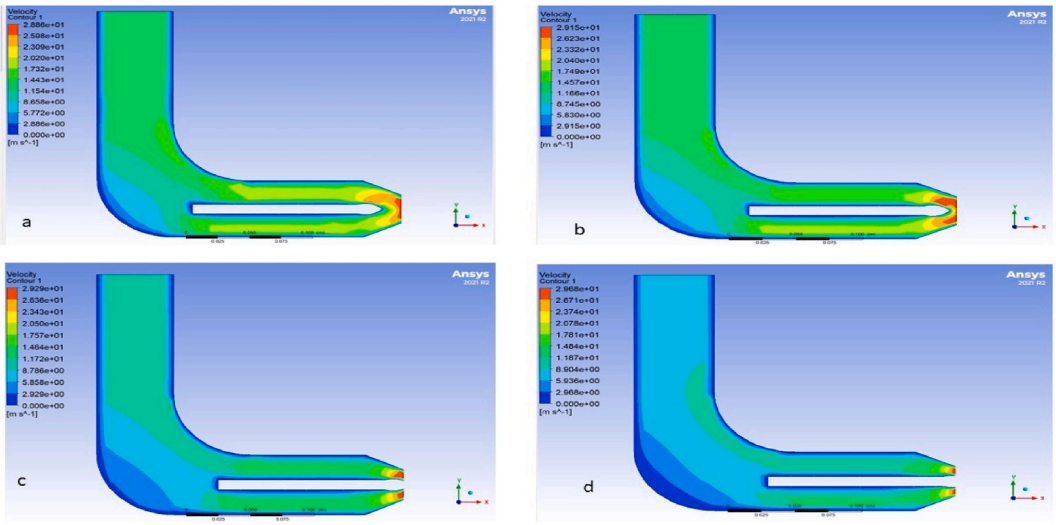

Fig. 2. Velocity contours based on spear locations: (a) 15 mm inside nozzle outlet (b) 5 mm inside nozzle outlet (c) spear tip coincides with the nozzle outlet (d) 5 mm outside the nozzle outlet.

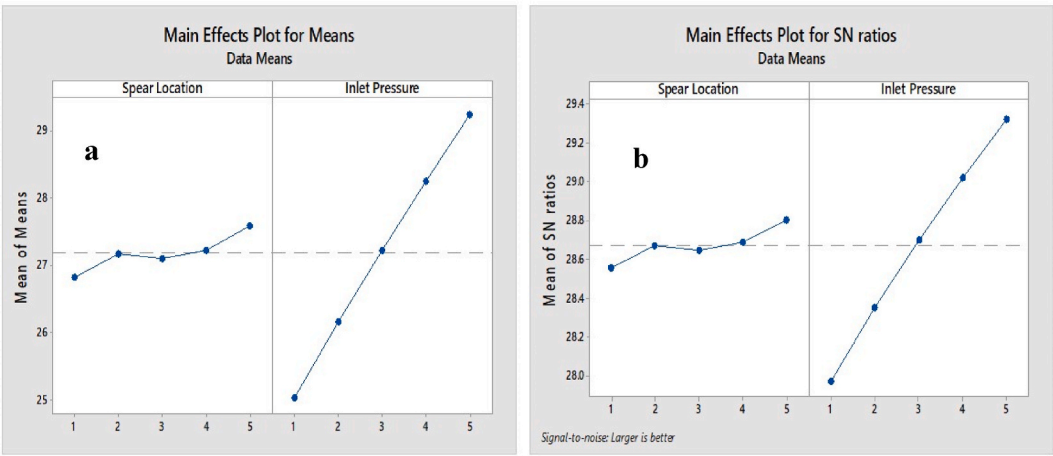

Fig. 3. Spear locations and inlet pressure: (a) Mean and (b) S/N ratio.

focuses on analysing the flow behaviour in the nozzle by varying input parameters (inlet pressure and spear location) and examining their influence on output parameters such as outlet pressure, outlet velocity, and tangential force components. Subsequently, the optimal influencing parameters were investigated for the corresponding variations of input parameters in terms of output parameters using Taguchi, TOPSIS, GRA and CRITIC analysis.

The Taguchi analysis was conducted, and the results were interpreted using the Signal-to Noise (S/N) ratio. The ratio establishes the relationship between the desired value (mean) and the undesired value (standard deviation) for the response [32,33]. S/N curves were generated based on the assigned boundary conditions of "the higher, the better," "the lower, the better," and "the medium, the better" for the input parameters.

The flow behaviour in the Pelton wheel nozzle was examined using response parameters such as velocity, pressure, and tangential force acting on the wheel. Among these parameters, velocity and tangential force are higher in the better case, whereas pressure is lower in the better situation. In the current work, the input parameters spear location and inlet pressure are variables. This analysis was done using Minitab software based on the mean of means, mean of S/N ratio, and ANOVA results. The Taguchi/ANOVA was performed individually for velocity behaviour, pressure behaviour, and tangential force component. On the Taguchi DoE Table 3, however, GRA and CRITIC analyses were carried out in the TOPSIS case. The comparison was made between TOPSIS and GRA combined and for ANOVA and CRITIC analysis combined.

After the Taguchi analysis, optimisation techniques such as TOPSIS, GRA, and CRITIC were performed. TOPSIS and GRA were run on the Taguchi DoE, and the findings were in good agreement [34] in terms of contribution percentage, and CRITIC results agreed well with Taguchi analysis and ANOVA.

Table 4
Analysis of Variance for SN ratios.

Source	DF	Seq SS	Adj SS	Adj MS	F	P	% of Contribution
Spear Location	4	0.15192	0.15192	0.03798	40680.22	0	2.613
Inlet Pressure	4	5.66144	5.66144	1.41536	1516004	0	97.386
Residual Error	16	0	0	0			
Total	24	5.81338					100

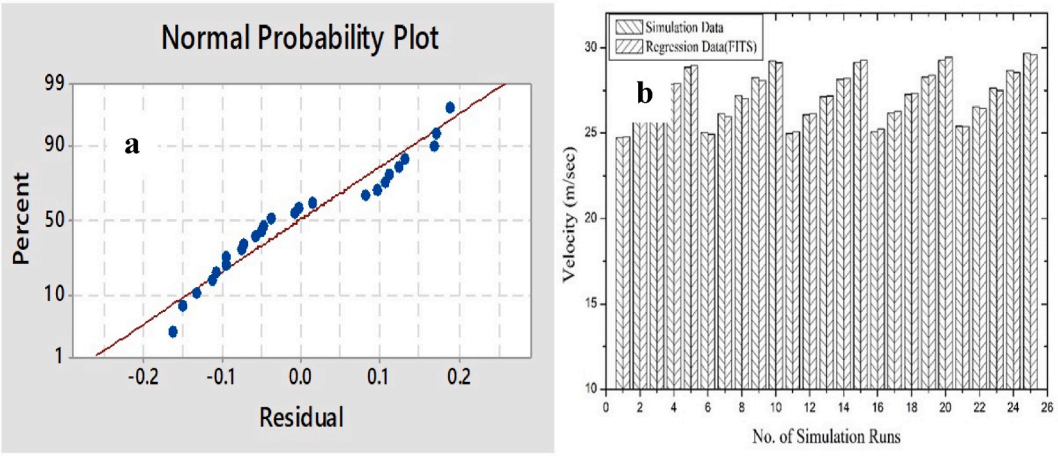

Fig. 4. Velocity properties: (a) Normal probability plot and (b) comparison between simulated data and its fits.

4.1. Taguchi analysis on velocity behaviour property

The velocity behaviour in the PW was investigated by varying parameters such as spear placement and inlet pressure. As the spear approaches closer to the nozzle exit, the outlet velocity steadily increases. The velocity parameter increases as the cross-sectional size of the nozzle decreases and pressure drops occur, as depicted in Fig. 2[a-d]. The variation in inlet pressure follows a similar pattern.

4.1.1. ANOVA analysis

Since Taguchi analysis was performed on the output velocity parameter, it is clear that the best values for velocity behavior are obtained for the first location and first input pressure as these values are close to zero, as shown in Fig. 3 (a –b). Among these two inlet variables (location of spear and inlet pressure), the 1st rank was obtained for pressure and next is the spear location as shown in Table 4. The percentage of contribution for velocity behaviour, the inlet pressure is 97.38%, and spear location is 2.613%, as indicated in Table 4. The velocity behaviour for five different spear locations increases with an increase in the inlet pressure, as shown in Fig. 3 (a–b), and simulated values have high accuracy with an R-square (R^2) value of 99.48%. The regression equation is developed based on the input variables like inlet pressure and spear location, as shown by Eq. (22).

The process parameter obtained from ANOVA affects the performance of the PT. From the ANOVA results, as shown in Tables 4 and it was found that inlet pressure is more significantly influenced by the velocity parameter and later followed by spear location. The percentage of contribution of inlet pressure and spear location was 97.386% and 2.613%, respectively, as shown in Table 4.

In the present work, linear regression analysis was performed using Minitab software, and a mathematical model was developed for velocity parameters with the function of inlet pressure and spear location. The equations obtained from regression analysis are shown in Eq. (22) for the velocity. The coefficient of determination (R^2) determines the capability of the developed mathematical model, and it varies between zero and one. If this R^2 value is close to one, it means that the variables are a good fit. In the present study of velocity behaviour in the PW, the developed regression model has an R^2 of 99.48%, which is a good fit with less error. Based on Fig. 4(a–b), it was observed that the residual values are very close to the straight line, which indicates that the developed mathematical model is more significant.

$$V_B = 23.56 + 0.1567SL + 1.0491IP \tag{22}$$

Where V_B, SL , and IP are the respective velocity behaviour (m/s), spear location (mm), and inlet pressure (Pa)

4.2. Taguchi analysis on pressure behaviour property

The inlet pressure is the most influential factor on the performance of the PW. Based on the simulation values, changing the inlet

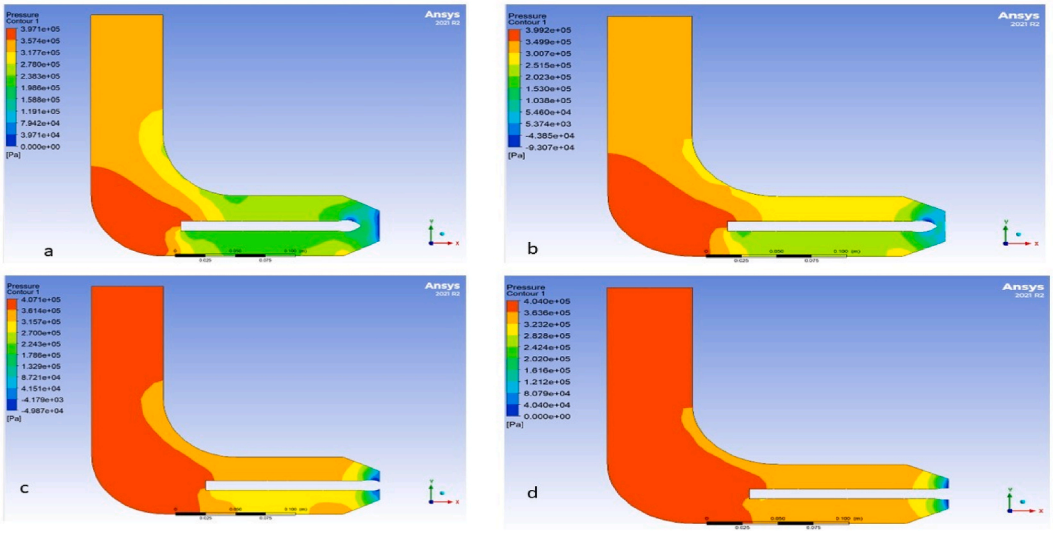

Fig. 5. Pressure contours based on spear locations (a) 15 mm inside nozzle outlet (b) 5 mm inside nozzle out let (c) spear tip coincides with the nozzle outlet (d) 5 mm outside the nozzle outlet.

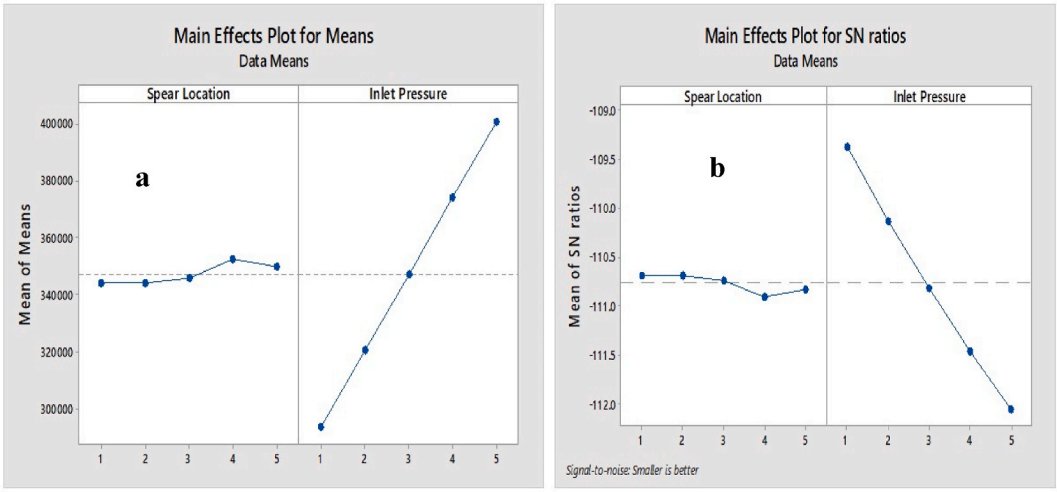

Fig. 6. Pressure behaviour in terms of the inlet pressure and spear location: (a) Means and (b) S/N ratio.

Table 5
Analysis of Variance for S/N ratios.

Source	DF	Seq SS	Adj SS	Adj MS	F	P	% of Contribution
Spear Location	4	0.1858	0.1858	0.04644	82356.09	0	0.813
Inlet Pressure	4	22.6639	22.6639	5.66597	10048443	0	99.187
Residual Error	16	0	0	0			
Total	24	22.8496					100

pressure and spear location resulted in a gradual change in the outlet pressure. As the inlet pressure increases, the outlet pressure of the PW decreases, as shown in Fig. 5(a–d). A similar trend was observed when changing the spear location. The reduced cross-sectional area in the PW nozzle, which leads to pressure drop and other factors, was caused by the minor losses in the pipe.

4.2.1. ANOVA analysis

Based on Fig. 6(a–b) generated by the Taguchi analysis, the best values of the pressure behaviour in terms of the inlet pressure and spear location are obtained for a starting spear location and initial inlet pressure value as these values are close to zero. However, these

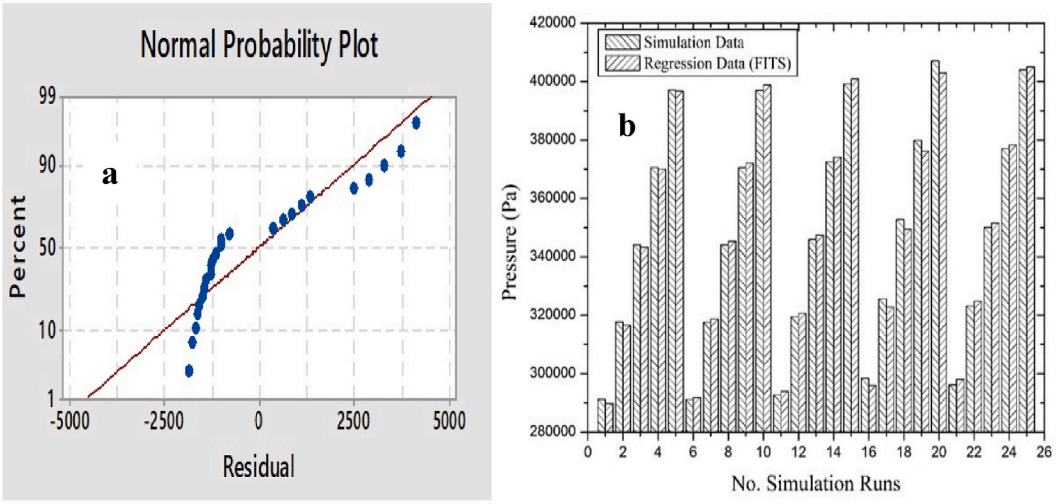

Fig. 7. Pressure behaviour data: (a) Normal Probability Plot and (b) Simulated pressure vs. no of runs for its fits.

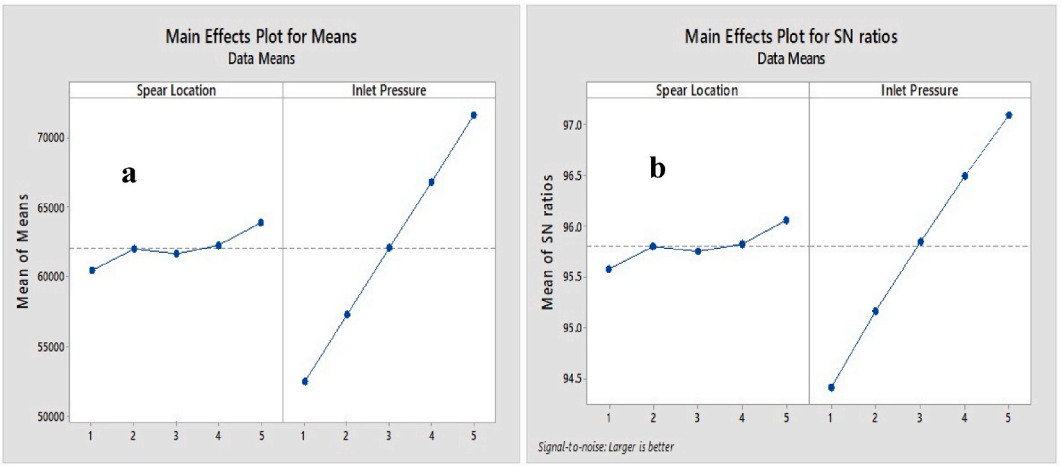

Fig. 8. Tangential force components of (a) Means and (b) S/N ratio for spear location and inlet pressure.

two parameters have an influence on the performance of the Pelton Wheel. As represented in Table 5, which was obtained from ANOVA, among the two factors (inlet pressure and spear location), the 1st rank was obtained for inlet pressure and the 2nd rank was obtained for spear location. In terms of the percentage of contribution, the inlet pressure was 99.187%, and the spear location was 0.813%. The inlet pressure is the important parameter, which directly depends on the performance of the PW. This pressure is developed by the pumps or pressure developed by the pressure head. Based on the simulation data, the outlet pressure decreases because the pressure and velocity are inversely proportional to each other.

The simulated data related to the pressure behaviour parameter were analyzed by ANOVA. The data had high accuracy as indicated by the R^2 value of 99.75%, which is very close to 100%. The developed mathematical model through regression analysis is represented by Eq. (23), with the response being outlet pressure and factors including inlet pressure and spear location. The analysis was carried out using Minitab software. The linear regression analysis was a module within ANOVA, allowing the determination of errors in the simulation data through the R^2 value. The R^2 value indicates the model's ability to define errors ranging from zero to one. The simulated data closely align with a straight line in the probability curve, as depicted in Fig. 7(a–b).

It was observed that the percentage of contribution obtained by ANOVA for pressure behaviour (99.18%) was higher compared to the velocity behaviour (97.38%) and tangential force component (97.38%) of the water jet from the nozzle. It was also noted that the velocity behaviour and tangential force component had the same level of contribution.

$$P_O = 261086 + 2058SL + 267191IP \tag{23}$$

where P_O is the outlet pressure (Pa)

Table 6
Analysis of variance for SN ratios.

Source	DF	Seq SS	Adj SS	Adj MS	F	P	% of Contribution
Spear Location	4	0.6077	0.6077	0.15192	40680.22	0	2.613
Inlet Pressure	4	22.6458	22.6458	5.66144	1516004	0	97.386
Residual Error	16	0.0001	0.0001	0			
Total	24	23.2535					100

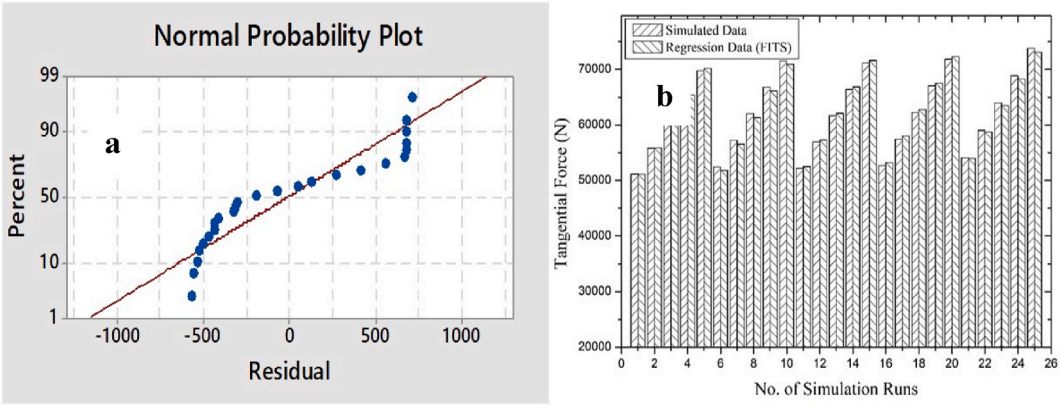

Fig. 9. Tangential force component of (a) Normal Probability Plot and (b) Comparison between simulated data and FITS data.

Table 7
TOPSIS analysis.

Simulation No.	Normalised Weighted matrix			Separation Matrix			Preference Value	Rank
	Outlet Pressure	Velocity	Tangential Force	Outlet Pressure	Velocity	Tangential Force		
1	0.073	0.020	0.073	0.073	0.020	0.073	0.4715	23
2	0.080	0.021	0.080	0.080	0.021	0.080	0.4670	24
3	0.087	0.022	0.087	0.087	0.022	0.087	0.4703	23
4	0.093	0.023	0.093	0.093	0.023	0.093	0.4844	18
5	0.100	0.024	0.100	0.100	0.024	0.100	0.4974	13
6	0.073	0.021	0.075	0.073	0.021	0.075	0.4875	16
7	0.080	0.022	0.082	0.080	0.022	0.082	0.4942	14
8	0.087	0.023	0.089	0.087	0.023	0.089	0.5090	9
9	0.093	0.023	0.096	0.093	0.023	0.096	0.5220	6
10	0.100	0.024	0.103	0.100	0.024	0.103	0.5248	5
11	0.074	0.021	0.075	0.074	0.021	0.075	0.4805	14
12	0.080	0.022	0.082	0.080	0.022	0.082	0.4829	12
13	0.087	0.022	0.088	0.087	0.022	0.088	0.4929	11
14	0.094	0.023	0.095	0.094	0.023	0.095	0.5068	7
15	0.100	0.024	0.102	0.100	0.024	0.102	0.5136	5
16	0.075	0.021	0.076	0.075	0.021	0.076	0.4731	10
17	0.082	0.022	0.082	0.082	0.022	0.082	0.4720	10
18	0.089	0.023	0.089	0.089	0.023	0.089	0.4812	9
19	0.096	0.023	0.096	0.096	0.023	0.096	0.4960	8
20	0.102	0.024	0.103	0.102	0.024	0.103	0.5050	6
21	0.075	0.021	0.078	0.075	0.021	0.078	0.4978	6
22	0.081	0.022	0.085	0.081	0.022	0.085	0.5127	5
23	0.088	0.023	0.092	0.088	0.023	0.092	0.5323	4
24	0.095	0.024	0.099	0.095	0.024	0.099	0.5396	1
25	0.102	0.025	0.106	0.102	0.025	0.106	0.5351	2

4.3. Tangential force component of jet developed by nozzle and Taguchi analysis

The PW is also known as a tangential flow impulse turbine because it convert water's potential energy into a water jet with kinetic energy. This kinetic energy helps to drive the Pelton runner. Therefore, the tangential force component was calculated from the water jet at the nozzle, which is a crucial parameter that generates impulse force acting on the buckets of the Pelton wheel runner and affects the PW's performance. This tangential force component was determined using velocity triangle concepts presented in Table 3.

Table 8
GRA analysis results.

Sim. No.	Normalisation			Deviation Sequence			GRA Coefficient			Average	Ranks
	Outlet Pres.	Vel.	Tag. Force	Outlet Pres.	Vel.	Tag. Force	Outlet Pres.	Vel.	Tag. Force		
1	1.00	0.00	0.00	0.00	1.00	1.00	1.00	0.33	0.33	0.555	9
2	0.77	0.22	0.21	0.23	0.78	0.79	0.69	0.39	0.39	0.488	22
3	0.54	0.43	0.41	0.46	0.57	0.59	0.52	0.47	0.46	0.483	23
4	0.31	0.64	0.62	0.69	0.36	0.38	0.42	0.58	0.57	0.523	15
5	0.09	0.84	0.82	0.91	0.16	0.18	0.35	0.75	0.74	0.615	5
6	1.00	0.06	0.06	0.00	0.94	0.94	1.00	0.35	0.35	0.565	6
7	0.77	0.29	0.27	0.23	0.71	0.73	0.69	0.41	0.41	0.502	15
8	0.54	0.50	0.48	0.46	0.50	0.52	0.52	0.50	0.49	0.505	14
9	0.31	0.71	0.69	0.69	0.29	0.31	0.42	0.63	0.62	0.558	6
10	0.09	0.91	0.90	0.91	0.09	0.10	0.35	0.85	0.84	0.680	3
11	0.99	0.05	0.05	0.01	0.95	0.95	0.97	0.35	0.34	0.554	6
12	0.76	0.28	0.26	0.24	0.72	0.74	0.67	0.41	0.40	0.494	13
13	0.53	0.49	0.47	0.47	0.51	0.53	0.51	0.49	0.48	0.497	11
14	0.30	0.69	0.67	0.70	0.31	0.33	0.42	0.62	0.61	0.547	7
15	0.07	0.89	0.88	0.93	0.11	0.12	0.35	0.82	0.81	0.662	3
16	0.94	0.07	0.07	0.06	0.93	0.93	0.89	0.35	0.35	0.529	6
17	0.70	0.30	0.28	0.30	0.70	0.72	0.63	0.42	0.41	0.484	9
18	0.47	0.51	0.49	0.53	0.49	0.51	0.48	0.51	0.50	0.496	8
19	0.23	0.72	0.70	0.77	0.28	0.30	0.39	0.64	0.63	0.555	4
20	0.00	0.92	0.91	1.00	0.08	0.09	0.33	0.86	0.85	0.684	2
21	0.96	0.14	0.13	0.04	0.86	0.87	0.92	0.37	0.36	0.551	3
22	0.72	0.37	0.35	0.28	0.63	0.65	0.64	0.44	0.43	0.507	4
23	0.49	0.59	0.56	0.51	0.41	0.44	0.50	0.55	0.53	0.526	3
24	0.26	0.80	0.78	0.74	0.20	0.22	0.40	0.71	0.70	0.604	2
25	0.03	1.00	1.00	0.97	0.00	0.00	0.34	1.00	1.00	0.780	1

Through Taguchi anlysis, theoretically calculated tangential force components yielded better values for the first spear location and the starting inlet pressure value, as depicted in Fig. 8(a and b). In terms of percentage contribution, the inlet pressure values had a higher contribution at 97.386% while the spear had a contribution of 2.613%, as shown in Table 6.

4.3.1. ANOVA analysis

Fig. 8(a-b) further shows that as the inlet pressure increases from one number to the next, the tangential force steadily increases for all spear locations. With an R^2 value of 99.45%, the estimated force values were highly accurate, and the mathematical regression model was expressed as Eq. (24). As shown in Fig. 9 (a-b), the probability graph and comparison of simulated and regression data reflect the reduced inaccuracy between them.

$$T_F = 45613 + 716.4SL + 4772.7IP \tag{24}$$

where T_F *is* the tangential force (N)

4.4. TOPSIS

TOPSIS analysis was performed on the Taguchi DoE, as highlighted in Table 7. The TOPSIS results were depicted in terms of rank sequence based on the response parameters (outlet pressure, velocity, and tangential force) and influencing factors (inlet pressure and spear placement). The TOPSIS ranks were produced using the preference value, separation weight matrix, and normalization weight matrix, displayed in Table 7. These values were obtained from Eqs. (1)–(8). The multi-objective optimal was converted to a single objective optimal by conducting the TOPSIS. The optimum solution can be determined based on the highest preference value, and that particular best performance can be expressed with the highest rank [16 and17]. As seen in Table 7, simulation run #24 had the best performance since it had the highest preference order and was the next ideal, followed by runs #25 and #23.

4.5. Grey relational analysis

The Grey Relational Analysis (GRA) was performed for the Taguchi DoE shown in Table 8. As previously stated, the input and output parameters of the simulation values were initially normalized. The Grey Relational Coefficient (GRC) was then computed. The simulated results were normalized using Eqs. (9) and (10), based on different input and output parameters, and the data is also displayed in Table 8. Using Eq. (11), the GRC for each output was determined, followed by the Grey Relation Grade (GRG). In order to maintain the ideal condition, the same weightage was maintained for fluid behaviour parameters at the nozzle, and GRG was utilized to describe overall performance, as shown in Table 8. By integrating the Taguchi analysis with GRA, the multi-objective optimal problem was reduced to a single-objective optimal issue [16,17]. The best results in terms of GRG and highest rank were represented for various input settings. As seen in Table 8, simulation run #25 had the highest rating, followed by #24 and #23. #25 achieved the

Table 9
CRITIC analysis.

	SMRLCC			SCC	SD	CQ	Objective Weights	Wt (%)	Ranks
	O_F	Ve	T_F						
Outlet pressure (O_F)	1.000	−0.991	−0.992	3.983	0.334	1.331	0.519	51.946	1
Outlet velocity	−0.991	1.000	1.000	1.992	0.309	0.616	0.240	24.044	2
Tangent force (T_F)	−0.992	1.000	1.000	1.992	0.309	0.615	0.240	24.011	3

highest GRA value, indicating the best overall performance.

4.6. Criteria Importance Through Intercriteria Correlation (CRITIC) Analysis

The weight normalized decision matrix was calculated using Eqs. (13)- (15), and the data is represented in Table 9. Based on the objective weights, the ranking was assigned and represented in Table 9. The most influencing parameter on the performance was the outlet pressure from the nozzle of the PW, as it had 51.94% of the objective weight (W_t), and the next influencing parameter was the tangential force component, which had 24.011%. The last influencing parameter was outlet velocity, which had 24.044% of the objective weight.

The Taguchi method was used to build the experimental design, and then Taguchi analysis was used to study the parameters such as velocity behaviour, pressure behaviour, and tangential force component. This research revealed that the most influential input variable (inlet pressure) had a greater influence on the output parameters, such as outlet pressure, outlet velocity, and tangential force component. ANOVA further demonstrated that the simulated data has a 99% confidence level for all output parameters.

The Taguchi DoE-based TOPSIS and GRA analysis were then used to forecast the optimum output affecting parameter on the simulated values. The TOPSIS and GRA both agree. The optimal simulation run for #24 and #25 was obtained. According to CRITIC analysis, the best influencing parameter on the overall performance of the PW is outlet pressure. Similarly, from the Taguchi analysis, the inlet pressure had the greatest influence on the performance of the PW, as shown in Tables 3–5.

5. Conclusion

This study evaluated the influence of significant input and output parameters on the performance of a Pelton wheel. For this purpose, four different types of optimisation techniques are implemented. Based on the Taguchi analysis, 97.38% of inlet pressure and 2.613% of spear location show an influence on the output velocity behaviour. The output pressure behavior and tangential force component followed a similar pattern. The TOPSIS analysis, with the combination of -5mm spear location, 386106 Pa of inlet pressure, 377033 Pa of outlet pressure, 28.67 m/s of outlet velocity, and tangential force component of 73772.92 N gives the best simulation run at #24. Similarly, for GRA analysis, the #25 simulation run is optimal, and both TOPSIS and GRA are in good agreement. By CRITIC analysis, the nozzle output parameters' influence on the performance of the Pelton wheel was examined. According to this analysis, the major contribution is observed for the outlet pressure (51.94%), followed by the nozzle outlet velocity (24.04%) and tangential force component. Taguchi analysis defines the influence of the input parameters, while TOPSIS and GRA methods provide a brief with the combination of input and output parameters. The CRITIC technique explains the influence of the output parameter, and finally, the regression analysis gives the accuracy level in the simulation data.

CRediT authorship contribution statement

Satish Geeri: Writing – original draft, Methodology, Conceptualization. **Aditya Kolakoti:** Software, Methodology, Formal analysis, Data curation, Conceptualization. **Olusegun David Samuel:** Writing – review & editing, Writing – original draft, Visualization, Project administration, Investigation, Conceptualization. **Mohamed Abbas:** Writing – review & editing, Investigation. **Peter Alenoghena Aigba:** Writing – review & editing, Visualization, Investigation. **Habeeb A. Ajimotokan:** Writing – review & editing, Investigation. **Christopher C. Enweremadu:** Writing – review & editing, Resources, Investigation. **Noureddine Elboughdiri:** Writing – review & editing, Investigation. **M.A. Mujtaba:** Writing – review & editing, Investigation.

Declaration of competing interest

The authors declare that they have no known competing financial interests or personal relationships that could have appeared to influence the work reported in this paper.

Acknowledgments

The authors extend their appreciation to the Deanship of Scientific Research at King Khalid University (KKU) for funding this research through the Research Group Program Under the Grant Number:(R.G.P.1/431/44).

Nomenclature

Adj MS	Adjusted mean squares
Adj SS	Adjusted sums of squares
CQ	Criterion quantity
E_{iJ}	Component of the rate of deformation
DF	Degree of freedom
D_m	Decision Matrix
$\xi_i(P)$	Grey relational coefficients
$X_i(P)$	Grey relational generation
γ_i	Grey Output response
IP	Inlet pressure
r_{ij}	Normalized matrix
P_O	Outlet pressure
P_i	Positive ideal Solution
SL	Spear location
SD	Standard deviation
SCC	Sum of the Conflict by Criterion
SMRLCC	Symmetric matrix with representation of Linear Correlation Coefficients
T_F	Tangential force
U	Weighted normalized decision matrix
μ_i	Velocity component in the corresponding direction
V_B	Velocity behaviour
Ve	Velocity
C_j	Weight Percentage

References

[1] A. Perrig, F. Avellan, J.L. Kueny, M. Fahrat, E. Parkinson, Flow in a Pelton turbine bucket: numerical and experimental investigations, J. Fluid Eng. 128 (2006).
[2] S. Oyedepo, Energy and sustainable development in Nigeria: the way forward, Energy, Sustainability and Society 2 (1) (2012) 1–17.
[3] M. Pita, T. Gaonnwe, Investigating the effect of pressure head on the efficiency of pelton wheel and Francis turbine, in: IEEE 13th International Conference on Mechanical and Intelligent Manufacturing Technologies (ICMIMT), 2022. Cape Town, South Africa.
[4] K. Patel, B. Patel, M. Yadav, T. Foggia, Development of Pelton turbine using numerical simulation, IOP Conf. Ser. Earth Environ. Sci. 12 (1) (2010) 012048.
[5] G. Aggidis, A. Židonis, Hydro turbine prototype testing and generation of performance curves: fully automated approach, Renew. Energy 71 (2014) 433–441.
[6] D. Nedelcu, V. Cojocaru, R. Avasiloaie, Numerical investigation of nozzle jet flow in a pelton microturbine, Machines 9 (8) (2021) 158.
[7] F. Stamatelos, J. Anagnostopoulos, D. Papantonis, Performance measurements on a Pelton turbine model, Proc. Inst. Mech. Eng. A J. Power Energy 225 (3) (2011) 351–362.
[8] M. Din, G. Harmain, Assessment of erosive wear of Pelton turbine injector: nozzle and spear combination–A study of Chenani hydro-power plant, Eng. Fail. Anal. 116 (2020) 104695.
[9] G.A. Aggidis, E. Luchinskaya, R. Rothschild, D.C. Howard, The costs of small-scale hydro power production: impact on the development of existing potential, Renew. Energy 35 (12) (2010) 2632–2638.
[10] O. Alomar, H. Abd, M. Salih, F. Ali, Performance analysis of Pelton turbine under different operating conditions: an experimental study, Ain Shams Eng. J. 13 (4) (2021) 101684.
[11] A. Kumar, R. Saini, Performance parameters of Savonius type hydrokinetic turbine–A Review, Renew. Sustain. Energy Rev. 64 (2016) 289–310.
[12] M.S. Khani, Y. Shahsavani, M. Mehraein, O. Kisi, Performance evaluation of the savonius hydrokinetic turbine using soft computing techniques, Renew. Energy (2023) 118906.
[13] R. Kumar, S. Sarkar, Effect of design parameters on the performance of helical Darrieus hydrokinetic turbines, Renew. Sustain. Energy Rev. 162 (2022) 112431.
[14] O. Leman, R. Wulandari, R. Bintara, Optimization of Nozzle Number, Nozzle Diameter and Number of Bucket of Pelton Turbine Using Computational Fluid Dynamics and Taguchi Methods, 2019.
[15] E. Gallego, A. Rubio-Clemente, J. Pineda, L. Velásquez, E. Chica, Experimental analysis on the performance of a pico-hydro Turgo turbine, Journal of King Saud University-Engineering Sciences 33 (4) (2021) 266–275.
[16] M.M. Kamal, R.P. Saini, A numerical investigation on the influence of savonius blade helicity on the performance characteristics of hybrid cross-flow hydrokinetic turbine, Renew. Energy 190 (2022) 788–804.
[17] A. Permanasari, P. Puspitasari, S. Utama, F. Yaqin, Experimental investigation and optimization of floating blade water wheel turbine performance using Taguchi method and analysis of variance (ANOVA), IOP Conf. Ser. Mater. Sci. Eng. 515 (1) (2019) 012086.
[18] Y. Ma, Y. Zhu, A. Zhang, C. Hu, S. Liu, Z. Li, Hydrodynamic performance of vertical axis hydrokinetic turbine based on Taguchi method, Renew. Energy 186 (2022) 573–584.
[19] Luis A. Gallo, Edwin L. Chica, Elkin G. Flórez, Numerical optimization of the blade profile of a savonius type rotor using the response surface methodology, Sustainability, MDPI 14 (9) (2022) 1–18.
[20] B. Zoppé, C. Pellone, T. Maître, P. Leroy, Flow analysis inside a Pelton turbine bucket, J. Turbomach. 128 (3) (2006) 500–511.
[21] C.M. Shashikumar, V. Madav, Numerical and experimental investigation of modified V-shaped turbine blades for hydrokinetic energy generation, Renew. Energy 177 (2021) 1170–1197.
[22] S. Wang, Q. Ma, Z. Guan, Measuring hospital efficiency in China using grey relational analysis and data envelopment analysis, in: International Conference on Grey Systems and Intelligent Services, 2007.
[23] D. Diakoulaki, G. Mavrotas, L. Papayannakis, Determining objective weights in multiple criteria problems: the critic method, Comput. Oper. Res. 22 (7) (1995) 763–770.
[24] Y. Wu, Z. Deng, Y. Tao, L. Wang, F. Liu, J. Zhou, Site selection decision framework for photovoltaic hydrogen production project using BWM-CRITIC-MABAC: a case study in Zhangjiakou, J. Clean. Prod. 324 (2021) 129233.

[25] S. Athreya, Y. Venkatesh, Application of Taguchi method for optimization of process parameters in improving the surface roughness of lathe facing operation, International Refereed Journal of Engineering and Science 1 (3) (2012) 13–19.
[26] C.M. Shashikumar, R. Honnasiddaiah, V. Hindasageri, V. Madav, Studies on application of vertical axis hydro turbine for sustainable power generation in irrigation channels with different bed slopes, Renew. Energy 163 (2021) 845–857.
[27] B. Popovski, A. Lipej, Z. Markov, P. Popovski, Optimisation of Pelton turbine jet deflector using CFD analysis, IOP Conf. Ser. Earth Environ. Sci. 240 (2) (2019) 022031.
[28] L. Vytvytskyi, B. Lie, Mechanistic model for Francis turbines in OpenModelica, IFAC-PapersOnLine 51 (2) (2018) 103–108.
[29] B. Launder, D. Spalding, Lectures in mathematical models of turbulence, Comput. Methods Appl. Mech. Eng. 3 (1972) 269–289.
[30] L. Han, G. Zhang, R. Gong, H. Wei, W. Li, Physics of Bad-Behaved Flow in 6-Nozzle Pelton Turbine Through Dynamic Simulation 240 (2) (2019).
[31] D. Barale, G. Limbardi, R.R. Arakerimath, Modelling and parametric fluid flow analysis (CFD) and effect on convergent nozzle used in pelton turbine, J. Emerg. Technol. Innov. Res. (JETIR) 3 (7) (2016) 24–30.
[32] A. Kolakoti, G and Satish, Biodiesel production from low-grade oil using heterogeneous catalyst: an optimisation and ANN modelling, Aust. J. Mech. Eng. 21 (11) (2023) 316–328.
[33] T. Singh, U. Rajak, O. Samuel, P. Chaurasiya, K. Natarajan, T. Verma, P. Nashine, Optimization of performance and emission parameters of direct injection diesel engine fuelled with microalgae Spirulina (L.)–Response surface methodology and full factorial method approach, Fuel 285 (2021) 119103.
[34] S. Satya, A. Kolakoti, R. Rao, Optimization of palm methyl ester and its effect on fatty acid compositions and cetane number, Mathematical models in engineering 5 (1) (2019) 25–34.